

## SONOCHEMISTRY AND SONOLUMINESCENCE

KENNETH S. SUSLICK AND LAWRENCE A. CRUM

### 1. INTRODUCTION

High-energy chemical reactions occur during the ultrasonic irradiation of liquids.<sup>1-6</sup> The chemical effects of ultrasound, however, do not come from a direct interaction with molecular species. The velocity of sounds in liquids is typically about 1500 m/s; ultrasound spans the frequencies of roughly 15 kHz to 1 GHz, with associated acoustic wavelengths of  $10-10^{-4}$  cm. These are not molecular dimensions. No direct coupling of the acoustic field with chemical species on a molecular level can account for sonochemistry or sonoluminescence. Instead, these phenomena derive principally from acoustic cavitation: the formation, growth, and implosive collapse of bubbles in a liquid. Cavitation serves as a means of concentrating the diffuse energy of sound. Bubble collapse induced by cavitation produces intense local heating, high pressures, and very short lifetimes. In clouds of cavitating bubbles, these hot spots<sup>7,8</sup> have equivalent temperatures of roughly 5000 K, pressures of about 2000 atm, and heating and cooling rates above  $10^9$  K/s.

Related phenomena occur with cavitation in liquid-solid systems. Near an extended solid surface, cavity collapse is nonspherical and drives high-speed jets of liquid into the surface.<sup>9</sup> This process can produce newly exposed, highly heated surfaces. Furthermore, during ultrasonic irradiation of liquid-powder slurries, cavitation and the shock waves it creates can accelerate solid particles to high velocities.<sup>10</sup> The resultant interparticle collisions are capable of inducing dramatic changes in surface morphology, composition, and reactivity.<sup>11</sup>

The chemical effects of ultrasound are diverse and include dramatic improvements in both stoichiometric

and catalytic reactions.<sup>12-15</sup> In some cases, ultrasonic irradiation can increase reactivity by nearly a million-fold.<sup>16</sup> The chemical effects of ultrasound fall into three areas: homogeneous sonochemistry of liquids, heterogeneous sonochemistry of liquid-liquid or liquid-solid systems, and sonocatalysis (which overlaps the first two). Chemical reactions are not generally seen in the ultrasonic irradiation of solids or solid-gas systems.

Sonoluminescence may be considered a special case of homogeneous sonochemistry; however, recent discoveries in this field have heightened interest in the phenomenon in and by itself.<sup>17,18</sup> New data on the duration of the sonoluminescence flash suggest that under the conditions of single-bubble sonoluminescence (SBSL), a shock wave may be created within the collapsing bubble with the capacity to generate enormous temperatures and pressures within the gas.

Acoustic cavitation provides the potential for creating exciting new physical and chemical conditions in otherwise cold liquids and results in an enormous concentration of energy. If one considers the energy density in an acoustic field that produces cavitation and that in the collapsed cavitation bubble, there is an amplification factor of over 11 orders of magnitude. The enormous local temperatures and pressures so created result in phenomena such as sonochemistry and sonoluminescence and provide a unique means for fundamental studies of chemistry and physics under extreme conditions.

### 2. MECHANISTIC ORIGINS OF SONOCHEMISTRY AND SONOLUMINESCENCE

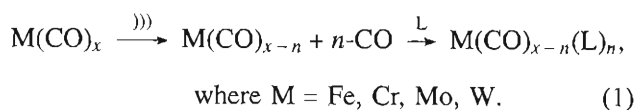
#### 2.1 Hot-Spot Formation during Cavitation

The most important acoustic process for sonochemistry and sonoluminescence is cavitation. Compression of a

gas generates heat. When the compression of cavities occurs in irradiated liquids, it is more rapid than thermal transport, which generates a short-lived, localized hot spot. There is a general consensus that this hot spot is the source of homogeneous sonochemistry. Rayleigh's early descriptions of a mathematical model for the collapse of cavities in incompressible liquids predicted enormous local temperatures and pressures.<sup>19</sup> Ten years later, Richards and Loomis reported the first chemical and biologic effects of ultrasound.<sup>20</sup> Alternative mechanisms involving electrical microdischarge have been occasionally proposed<sup>21,22</sup> but remain a minority viewpoint.

## 2.2 Two-Site Model of Sonochemical Reactivity

The transient nature of the cavitation event precludes conventional measurement of the conditions generated during bubble collapse. Chemical reactions themselves, however, can be used to probe reaction conditions. The effective temperature realized by the collapse of clouds of cavitating bubbles can be determined by the use of competing unimolecular reactions whose rate dependencies on temperature have already been measured. This technique of *comparative-rate chemical thermometry* was used by Suslick, Hammerton, and Cline to first determine the effective temperature reached during cavity collapse.<sup>7</sup> The sonochemical ligand substitutions of volatile metal carbonyls were used as these comparative-rate probes [Eq. (1), where the arrow with three small closing parentheses on top represents ultrasonic irradiation of a solution and L represents a substituting ligand]:



These kinetic studies revealed that there were in fact *two* sonochemical reaction sites: the first (and dominant site) is the bubble's interior gas phase while the second is an *initially* liquid phase. The latter corresponds either to heating of a shell of liquid around the collapsing bubble or to droplets of liquid ejected into the hot spot by surface wave distortions of the collapsing bubble.

The effective local temperatures in both sites were determined. By combining the relative sonochemical reaction rates for Eq. (1) with the known temperature behavior of these reactions, the conditions present during cavity collapse could then be calculated. The effective temperature of these hot spots was measured at  $\approx 5200$  K in the gas-phase reaction zone and  $\approx 1900$  K in the initially liquid zone.<sup>7</sup> Of course, the comparative-rate data represent only a composite temperature: During the

collapse, the temperature has a highly dynamic profile as well as a spatial temperature gradient. This two-site model has been confirmed with other reactions,<sup>23,24</sup> and alternative measurements of local temperatures by sonoluminescence are also consistent,<sup>8</sup> as discussed later.

## 2.3 Microjet Formation during Cavitation at Liquid–Solid Interfaces

Cavitation near extended liquid–solid interfaces is very different from cavitation in pure liquids. There are two proposed mechanisms for the effects of cavitation near surfaces: microjet impact and shock wave damage. Whenever a cavitation bubble is produced near a boundary, the asymmetry of the liquid particle motion during cavity collapse induces a deformation in the cavity.<sup>9</sup> The potential energy of the expanded bubble is converted into kinetic energy of a liquid jet that extends through the bubble's interior and penetrates the opposite bubble wall. Because most of the available energy is transferred to the accelerating jet, rather than the bubble wall itself, this jet can reach velocities of hundreds of meters per second. Because of the induced asymmetry, the jet often impacts the local boundary and can deposit enormous energy densities at the site of impact. Such energy concentration can result in severe damage to the boundary surface. Figure 1 shows a photograph of a jet developed in a collapsing cavity; Fig. 2 shows a micrograph of an impact site. The second mechanism of cavitation-induced surface damage invokes shock waves created by cavity col-

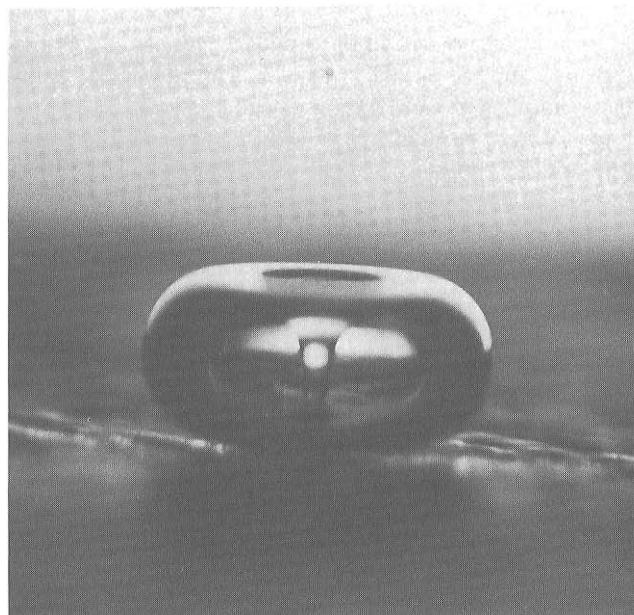


**Fig. 1** Photograph of liquid jet produced during collapse of a cavitation bubble. The width of the bubble is about 1 mm.

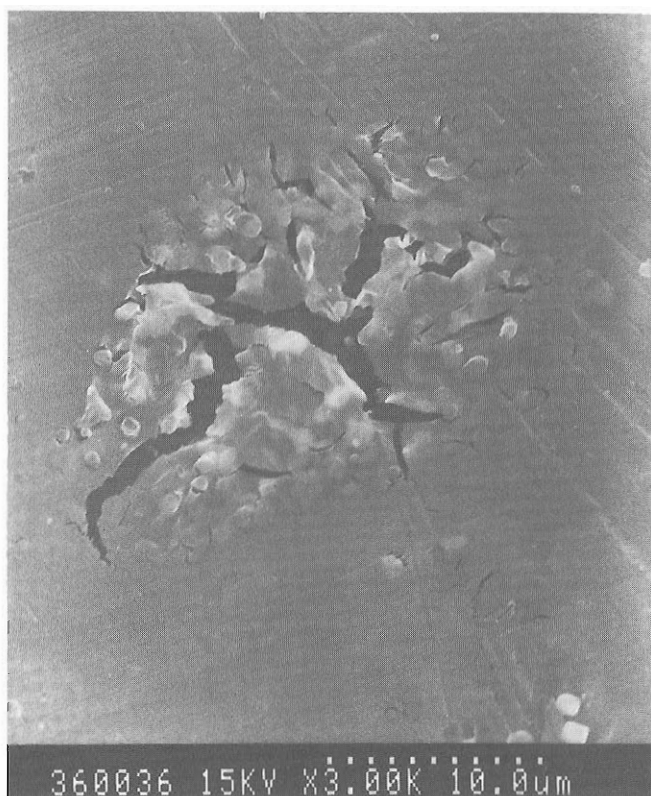


**Fig. 2** Photomicrograph of a region of an aluminum foil (about  $50\ \mu\text{m}$  in thickness) exposed to collapsing cavitation bubbles produced by extracorporeal shock wave lithotripter.

lapse in the liquid. The impingement of microjets and shock waves on the surface creates the localized erosion responsible for ultrasonic cleaning and many of the sonochemical effects on heterogeneous reactions. The erosion of metals by cavitation generates newly exposed, highly heated surfaces. Further details of jet and shock wave production and associated effects are presented elsewhere.<sup>25-27</sup>

Distortions of bubble collapse require a surface several times larger than the resonance bubble size. Thus, for solid particles smaller than  $\approx 200\ \mu\text{m}$ , damage associated with jet formation cannot occur with ultrasonic frequencies of  $\approx 20\ \text{kHz}$ . In these cases, however, the shock waves created by homogeneous cavitation can create high-velocity interparticle collisions.<sup>10,11</sup> Suslick and co-workers have found that the turbulent flow and shock waves produced by intense ultrasound can drive metal particles together at sufficiently high speeds to induce effective melting in direct collisions (Fig. 3) and the abrasion of surface crystallites in glancing impacts (Fig. 4). A series of transition-metal powders were used to probe the maximum temperatures and speeds reached during interparticle collisions. Using the irradiation of Cr, Mo, and W powders in decane at  $20\ \text{kHz}$  and  $50$

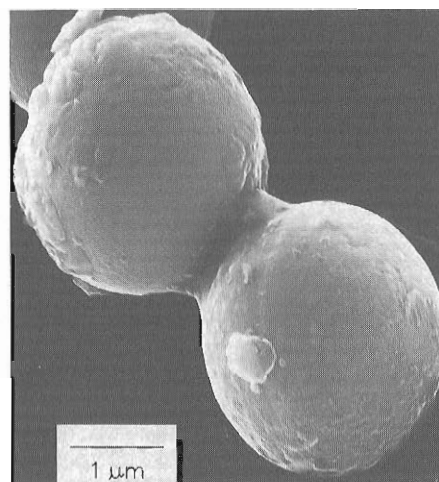


**Fig. 3** Scanning electron micrograph of Zn powder after ultrasonic irradiation for 30 min at  $288\ \text{K}$  in decane under Ar at  $20\ \text{kHz}$  and  $\approx 50\ \text{W}/\text{cm}^2$ . (Reproduced from Ref. 10 with permission.)

$\text{W}/\text{cm}^2$ , agglomeration and essentially a localized melting occur for the first two metals but not the third. On the basis of the melting points of these metals, the effective transient temperature reached at the point of impact during interparticle collisions is roughly  $3000^\circ\text{C}$ . From the volume of the melted region of impact, the amount of energy generated during collision was determined. From this, a lower estimate of the velocity of impact is roughly one-half the speed of sound.<sup>10</sup> These are precisely the effects expected on suspended particulates from cavitation-induced shock waves in the liquid.

### 3 SONOCHEMISTRY

High-intensity ultrasonic probes ( $50\text{--}500\ \text{W}/\text{cm}^2$ ) are the most reliable and effective source for laboratory-scale sonochemistry and are commercially available from several sources. Lower acoustic intensities can often be used

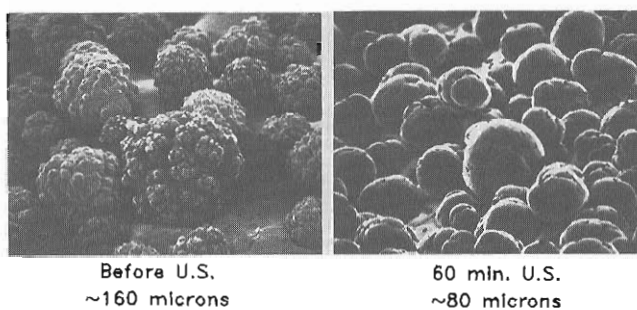


**Fig. 4** Effect of ultrasonic irradiation on surface morphology of Ni powder. (Reproduced from Ref. 16 with permission.)

in liquid–solid heterogeneous systems, because of the reduced liquid tensile strength at the liquid–solid interface. For such reactions, a common ultrasonic cleaning bath will therefore often suffice. The low intensity available in these devices ( $\approx 1 \text{ W/cm}^2$ ), however, can prove limiting. In addition, the standing-wave patterns in ultrasonic cleaners require accurate positioning of the reaction vessel. On the other hand, ultrasonic cleaning baths are easily accessible, relatively inexpensive, and usable on a moderately large scale. Finally, for larger scale irradiation, flow reactors with high ultrasonic intensities are commercially available in modular units of  $\approx 20 \text{ kW}$ .

### 3.1 Comparison of Cavitation Conditions to Other Forms of Chemistry

Chemistry is the study of the interaction of energy and matter. Chemical reactions require energy, in one form or another, to proceed: Chemistry stops as the temperature approaches absolute zero. One has only limited control, however, over the nature of this interaction. In large part, the properties of a specific energy source determines the course of a chemical reaction. Ultrasonic irradiation differs from traditional energy sources (such as heat, light, or ionizing radiation) in duration, pressure, and energy per molecule. The immense local temperatures and pressures and the extraordinary heating and cooling rates generated by cavitation bubble collapse mean that ultrasound provides an unusual mechanism for generating high-energy chemistry. Similar to photochemistry, very large amounts of energy are introduced in a short period of time, but it is thermal, not electronic, excitation. As in flash pyrolysis, high thermal temperatures are reached, but the duration is very much shorter (by more than  $10^4$ ) and the temperatures are even higher (by 5- to 10-fold). Similar to shock-tube chemistry or multiphoton infrared laser photolysis, cavitation heating is very short lived but occurs within condensed phases. Furthermore, sonochemistry has a high-pressure component, which suggests that one might be able to produce on a microscopic scale the same macroscopic conditions of high temperature–pressure “bomb” reactions or explosive shock wave synthesis in solids.

Control of sonochemical reactions is subject to the same limitation that any thermal process has: The Boltzmann energy distribution means that the energy per individual molecule will vary widely. One does have easy control, however, over the intensity of heating generated by acoustic cavitation through the use of various physical parameters (including thermal conductivity of dissolved gases, solvent vapor pressure inside the bubble, and ambient pressure). In contrast, frequency appears to be less important, at least within the range where cavita-

tion can occur (a few hertz to a few megahertz), although there have been few detailed studies of its role.

### 3.2 Homogeneous Sonochemistry: Bond Breaking and Radical Formation

The chemical effects of ultrasound on aqueous solutions have been studied for many years. The primary products are  $\text{H}_2$  and  $\text{H}_2\text{O}_2$ ; other high-energy intermediates have been suggested, including  $\text{HO}_2$ ,  $\text{H}^\cdot$ ,  $\text{OH}^\cdot$ , and perhaps  $e_{(\text{aq})}^-$ . The elegant work of Riesz and collaborators used electron paramagnetic resonance with chemical spin-traps to demonstrate definitively the generation of  $\text{H}^\cdot$  and  $\text{OH}^\cdot$  during ultrasonic irradiation, even with clinical sources of ultrasound.<sup>28</sup> The extensive work in Henglein’s laboratory involving aqueous sonochemistry of dissolved gases has established clear analogies to combustion processes.<sup>23,24</sup> As one would expect, the sonolysis of water, which produces both strong reductants and oxidants, is capable of causing secondary oxidation and reduction reactions, as often observed by Margulis and co-workers.<sup>29</sup>

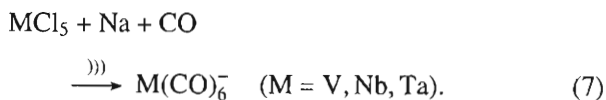
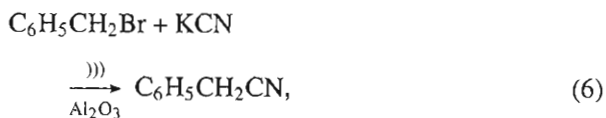
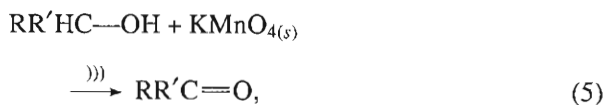
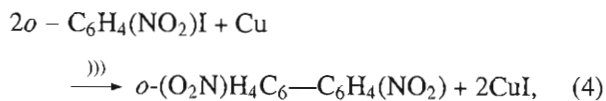
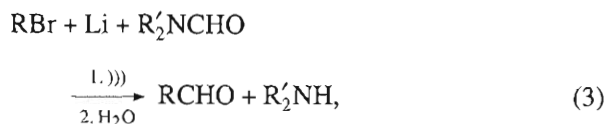
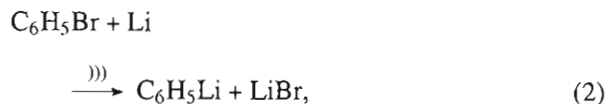
In contrast, the ultrasonic irradiation of organic liquids has been less studied. Suslick and co-workers established that virtually all organic liquids will generate free radicals upon ultrasonic irradiation, as long as the total vapor pressure is low enough to allow effective bubble collapse.<sup>30</sup> The sonolysis of simple hydrocarbons (e.g., *n*-alkanes) creates the same kinds of products associated with very high temperature pyrolysis. Most of these products ( $\text{H}_2$ ,  $\text{CH}_4$ , and the smaller *l*-alkenes) derive from a well-understood radical chain mechanism.

The sonochemistry of solutes dissolved in organic liquids also remains largely unexplored. The sonochemistry of metal carbonyl compounds is an exception.<sup>31</sup> Detailed studies of these systems led to important mechanistic understandings of the nature of sonochemistry. A variety of unusual reactivity patterns have been observed during ultrasonic irradiation, including multiple ligand dissociation, novel metal cluster formation, and the initiation of homogeneous catalysis (discussed later) at low ambient temperature, with rate enhancements greater than 100,000-fold.

Of special interest is the recent development of sonochemistry as a synthetic tool for the creation of unusual materials.<sup>32</sup> As one example is the recent discovery of a simple sonochemical synthesis of amorphous and nanostructured materials, including transition metals, alloys, carbides, and oxides.<sup>33</sup> A second example is the sonochemical preparation of protein microspheres,<sup>34</sup> which have applications for medical diagnostic imaging, drug delivery, and blood substitutes.

### 3.3 Heterogeneous Sonochemistry: Reactions of Solids with Liquids

The use of high-intensity ultrasound to enhance the reactivity of metals as stoichiometric reagents has become a routine synthetic technique for many heterogeneous organic and organometallic reactions,<sup>12-15</sup> especially those involving reactive metals, such as Mg, Li, or Zn. This development originated from the early work of Renaud and the more recent breakthroughs of Luche.<sup>12</sup> The effects are quite general and apply to reactive inorganic salts and to main-group reagents as well.<sup>35</sup> Less work has been done with unreactive metals (e.g., V, Nb, Mo, W), but results here are promising as well.<sup>11</sup> Rate enhancements of more than 10-fold are common, yields are often substantially improved, and byproducts are avoided. A few simple examples of synthetic applications of heterogeneous sonochemistry are shown in Eqs. (2)–(7), taken from the work of Ando, Boudjouk, Luche, Mason, and Suslick, among others:



The mechanism of the sonochemical rate enhancements in both stoichiometric and catalytic reactions of metals is associated with dramatic changes in morphology of both large extended surfaces and powders. As discussed earlier, these changes originate from microjet impact on large surfaces and high-velocity interparticle collisions in slurries. Surface composition studies by Auger electron spectroscopy and sputtered neutral mass spectrometry reveal that ultrasonic irradiation

effectively removes surface oxide and other contaminating coatings.<sup>11</sup> The removal of such passivating coatings can dramatically improve reaction rates. The reactivity of clean metal surfaces also appears to be responsible for the greater tendency for heterogeneous sonochemical reactions to involve single electron transfer rather than acid–base chemistry.<sup>36</sup>

Green, Suslick, and co-workers examined another application of sonochemistry to difficult heterogeneous systems: the process of molecular intercalation.<sup>37</sup> The adsorption of organic or inorganic compounds as guest molecules between the atomic sheets of layered inorganic solid hosts permits the systematic change of optical, electronic, and catalytic properties for a variety of technologic applications (e.g., lithium batteries, hydrodesulfurization catalysts, and solid lubricants). The kinetics of intercalation, however, are generally extremely slow, and syntheses usually require high temperatures and very long reaction times. High-intensity ultrasound dramatically increases the rates of intercalation (by as much as 200-fold) of a wide range of compounds into various layered inorganic solids (such as  $\text{ZrS}_2$ ,  $\text{V}_2\text{O}_5$ ,  $\text{TaS}_2$ ,  $\text{MoS}_2$ , and  $\text{MoO}_3$ ). Scanning electron microscopy of the layered solids coupled to chemical kinetics studies demonstrated that the origin of the observed rate enhancements comes from particle fragmentation (which dramatically increases surface areas) and to a lesser extent from surface damage. The ability of high-intensity ultrasound to rapidly form uniform dispersions of micrometer-sized powders of brittle materials is often responsible for the activation of heterogeneous reagents, especially nonmetals.

### 3.4 Sonocatalysis

Catalytic reactions are of enormous importance in both laboratory and industrial applications. Catalysts are generally divided into two types. If the catalyst is a molecular or ionic species dissolved in a liquid, then the system is *homogeneous*; if the catalyst is a solid, with the reactants either in a percolating liquid or gas, then it is *heterogeneous*. In both cases, it is often a difficult problem either to activate the catalyst or to keep it active.

Ultrasound has potentially important applications in both homogeneous and heterogeneous catalytic systems. The inherent advantages of sonocatalysis include (1) the use of low ambient temperatures to preserve thermally sensitive substrates and to enhance selectivity, (2) the ability to generate high-energy species difficult to obtain from photolysis or simple pyrolysis, and (3) the mimicry of high-temperature and high-pressure conditions on a microscopic scale.

Homogeneous catalysis of various reactions often

uses organometallic compounds. The starting organometallic compound, however, is often catalytically inactive until the loss of metal-bonded ligands (such as carbon monoxide) from the metal. Having demonstrated that ultrasound can induce ligand dissociation, the initiation of homogeneous catalysis by ultrasound becomes practical. A variety of metal carbonyls upon sonication will catalyze the isomerization of *l*-alkenes to the internal alkenes,<sup>31</sup> through reversible hydrogen atom abstraction, with rate enhancements of as much as  $10^5$  over thermal controls.

Heterogeneous catalysis is generally more industrially important than homogeneous systems. For example, virtually all of the petroleum industry is based on a series of catalytic transformations. Heterogeneous catalysts often require rare and expensive metals. The use of ultrasound offers some hope of activating less reactive, but also less costly, metals. Such effects can occur in three distinct stages: (1) during the formation of supported catalysts, (2) activation of preformed catalysts, or (3) enhancement of catalytic behavior during a catalytic reaction. Some early investigations of the effects of ultrasound on heterogeneous catalysis can be found in the Soviet literature.<sup>38</sup> In this early work, increases in turnover rates were usually observed upon ultrasonic irradiation but were rarely more than 10-fold. In the cases of modest rate increases, it appears likely that the cause is increased effective surface area; this is especially important in the case of catalysts supported on brittle solids.<sup>39</sup> More impressive accelerations, however, have included hydrogenations and hydrosilations by Ni powder, Raney Ni, and Pd or Pt on carbon.<sup>13</sup> For example, Casadonte and Suslick discovered that hydrogenation of alkenes by Ni powder is enormously enhanced ( $>10^5$ -fold) by ultrasonic irradiation.<sup>16</sup> This dramatic increase in catalytic activity is due to the formation of uncontaminated metal surfaces from interparticle collisions caused by cavitation-induced shock waves.

## 4 SONOLUMINESCENCE

Ultrasonic irradiation of liquids can also produce light. This phenomenon, known as sonoluminescence, was first observed from water in 1934 by Frenzel and Schultes.<sup>40</sup> As with sonochemistry, sonoluminescence derives from acoustic cavitation. Although sonoluminescence from aqueous solutions has been studied in some detail, only recently has significant work on sonoluminescence from nonaqueous liquids been reported.

### 4.1 Types of Sonoluminescence

It is now generally thought that there are two separate forms of sonoluminescence: multiple-bubble sonolumi-

nescence (MBSL) and single-bubble sonoluminescence (SBSL). When an acoustic field of sufficient intensity is propagated through a liquid, placing it under dynamic tensile stress, microscopic preexisting inhomogeneities act as nucleation sites for liquid rupture. This cavitation inception process results in many separate and individual cavitation events that would be distributed broadly throughout the acoustic field, especially if the liquid had a sufficiently large number of nuclei. Since most liquids such as water, have many thousands of potential nucleation sites per milliliter, the "cavitation field" generated by a propagating (or standing) acoustic wave typically consists of many bubbles, and is distributed over an extended region of space. If this cavitation is sufficiently intense to produce sonoluminescence, then we call this phenomenon multiple-bubble sonoluminescence.<sup>17,41</sup>

When an acoustic standing wave is excited within a liquid, pressure nodes and antinodes are generated. If a gas bubble is inserted into this standing wave, it will experience an acoustic force that will tend to force the bubble either to the node or antinode, depending upon whether it is respectively larger or smaller than its resonance size. Under the appropriate conditions, this acoustic force can balance the buoyancy force and the bubble is said to be "acoustically levitated." Such a bubble is typically quite small, compared to a wavelength (e.g., at 20 kHz, the resonance size is approximately  $150 \mu\text{m}$ ), and thus the dynamic characteristics of this bubble can often be examined in considerable detail, both from a theoretical and an experimental perspective.

It was recently discovered that under rather specialized but easily obtainable conditions a single, stable, oscillating gas bubble can be forced into such large-amplitude pulsations that it produces sonoluminescence emissions each (and every) acoustic cycle.<sup>42,43</sup> This phenomenon is called single-bubble sonoluminescence and has received considerable recent attention.<sup>17,18,44,45</sup>

### 4.2 Applications of MBSL to Measurements of Cavitation Thresholds

When the acoustic pressure amplitude of a propagating acoustic wave is relatively large (greater than  $\approx 0.5$  MPa) local inhomogeneities in the liquid often give rise to the explosive growth of a nucleation site to a cavity of macroscopic dimensions, primarily filled with vapor. Such a cavity is inherently unstable, and its subsequent collapse can result in an enormous concentration of energy. This violent cavitation event has been termed *transient* or *inertial cavitation* because the collapse of the cavity is primarily dominated by inertial forces.<sup>46</sup> A normal consequence of this rapid growth and violent collapse is that the cavitation bubble itself is destroyed. Although gas-filled residues from the collapse may give rise to reinitiation of the process, this type of cavitation is

thought to be a temporally discrete phenomenon. When one examines the light emissions from transient inertial cavitation, one can see single isolated events associated (presumably) with individual collapses of imploding cavities.

Because acoustic cavitation is often associated with large energy concentrations and thus potentially damaging mechanical effects, its presence is often undesirable (e.g., in the use of diagnostic ultrasound for prenatal examinations). Since light can be detected at very low levels and with very high time resolution, sonoluminescence can be used as a sensitive indicator of violent acoustic cavitation.<sup>47,48</sup> This capability permits threshold determination of cavitation inception for acoustic pulses of short time duration, as often is the case for medical ultrasound.

The widespread use of medical ultrasound has made possible enormous advances in the noninvasive examination of internal organs and conditions. With these diagnostic devices, the acoustic pulses used to create images are often less than a microsecond in length and possess duty cycles on the order of 1:1000. Since the acoustic pressure amplitudes generated by these devices are relatively large, it has been possible to use sonoluminescence as a detection criterion for acoustic cavitation generated by microsecond-length pulses of ultrasound. These studies have indicated that cavitation can be generated by acoustic pulses similar to those used in diagnostic ultrasound instruments and that continued studies need to be undertaken to evaluate the potential risks of these devices.<sup>49</sup>

### 4.3 Origin of MBSL Emissions: Chemiluminescence

The spectrum of MBSL in water consists of a peak at 310 nm and a broad continuum throughout the visible region. An intensive study of aqueous MBSL was conducted by Verrall and Sehgal.<sup>50</sup> The emission at 310 nm is from excited-state OH<sup>\*</sup>, but the continuum is difficult to interpret. The MBSL from aqueous and alcohol solutions of many metal salts have been reported and are characterized by emission from metal atom excited states.<sup>51</sup>

Flint and Suslick reported the first MBSL spectra of organic liquids.<sup>52</sup> With various hydrocarbons, the observed emission is from excited states of C<sub>2</sub> (d<sup>3</sup>Π<sub>g</sub>-a<sup>3</sup>Π<sub>u</sub>, the Swan lines), the same emission seen in flames. Furthermore, the ultrasonic irradiation of alkanes in the presence of N<sub>2</sub> (or NH<sub>3</sub> or amines) gives emission from CN excited states, but not from N<sub>2</sub> excited states. Emission from N<sub>2</sub> excited states would have been expected if the MBSL originated from microdischarge, whereas CN emission is typically observed from thermal sources. When oxygen is present, emission from excited

states of CO<sub>2</sub>, CH<sup>\*</sup>, and OH<sup>\*</sup> is observed, again similar to flame emission.

For both aqueous and nonaqueous liquids, MBSL is caused by chemical reactions of high-energy species formed during cavitation by bubble collapse. Its principal source is most probably not blackbody radiation or electrical discharge. The MBSL is a form of chemiluminescence.

### 4.4 Origin of SBSL Emissions: Imploding Shock Waves

It is known that the spectra of MBSL and SBSL are measurably different. For example, an aqueous solution of NaCl shows evidence of excited states of both OH<sup>\*</sup> and Na in the MBSL spectrum; however, the SBSL spectrum of an identical solution shows no evidence of either of these peaks.<sup>53</sup> Similarly, the MBSL spectrum falls off at low wavelengths, while the SBSL spectrum continues to rise, at least for bubbles containing most noble gases.<sup>54</sup>

Perhaps the most intriguing aspect of SBSL is the extremely short duration of the sonoluminescence flash. Putterman and his colleagues, using the fastest photomultiplier tube (PMT) available, determined that this duration must be at least as short as 50 ps, perhaps even lower.<sup>55</sup> Moran et al., using a streak camera, presented evidence of a 12-ps flash duration.<sup>56</sup> Because these measurements test the limitations of current technology, an accurate assessment of this pulse duration cannot be reliably given at this time.

As described earlier, the most likely explanation for the origin of sonoluminescence is the hot-spot theory, in which the potential energy given the bubble as it expands to maximum size is concentrated into a heated gas core as the bubble implodes. To understand the origin of sonoluminescence emissions, it is necessary first to understand something about the bubble dynamics that describe the bubble's motion. The equation that describes the oscillations of a gas bubble driven by an acoustic field is known generally by the name *Rayleigh-Plesset*, one form of which, called the *Gilmore equation*, can be expressed as a second-order nonlinear differential equation given as

$$R \left( 1 - \frac{U}{C} \right) \frac{d^2 R}{dt^2} + \frac{3}{2} \left( 1 - \frac{U}{3C} \right) \left( \frac{dR}{dt} \right)^2 - \left( 1 + \frac{U}{C} \right) H - \frac{R}{C} \left( 1 - \frac{U}{C} \right) \frac{dH}{dt} = 0. \quad (8)$$

The radius and velocity of the bubble wall are given by  $R$  and  $U$ , respectively. The values for  $H$ , the enthalpy at the bubble wall, and  $C$ , the local sound speed, may be expressed as follows using the Tait equation of state for

the liquid:

$$H = \frac{n}{n-1} \frac{A^{1/n}}{\rho_0} \left\{ (P(R) + B)^{(n-1)/n} - [P_\infty(t) + B]^{(n-1)/n} \right\}, \quad (9)$$

$$C = [c_0^2 + (n-1)H]. \quad (10)$$

The linear speed of sound in the liquid is  $c_0$ . The constants  $A$ ,  $B$ , and  $n$  should be set to the appropriate values for water. Any acoustic forcing function is included in the pressure at infinity,  $P_\infty(t)$ . The pressure at the bubble wall,  $P(R)$ , is given by

$$P(R) = \left( P_0 + \frac{2\sigma}{R} \right) \left( \frac{R_0}{R} \right)^{3\gamma} - \frac{2\sigma}{R} - \frac{4\mu U}{R}, \quad (11)$$

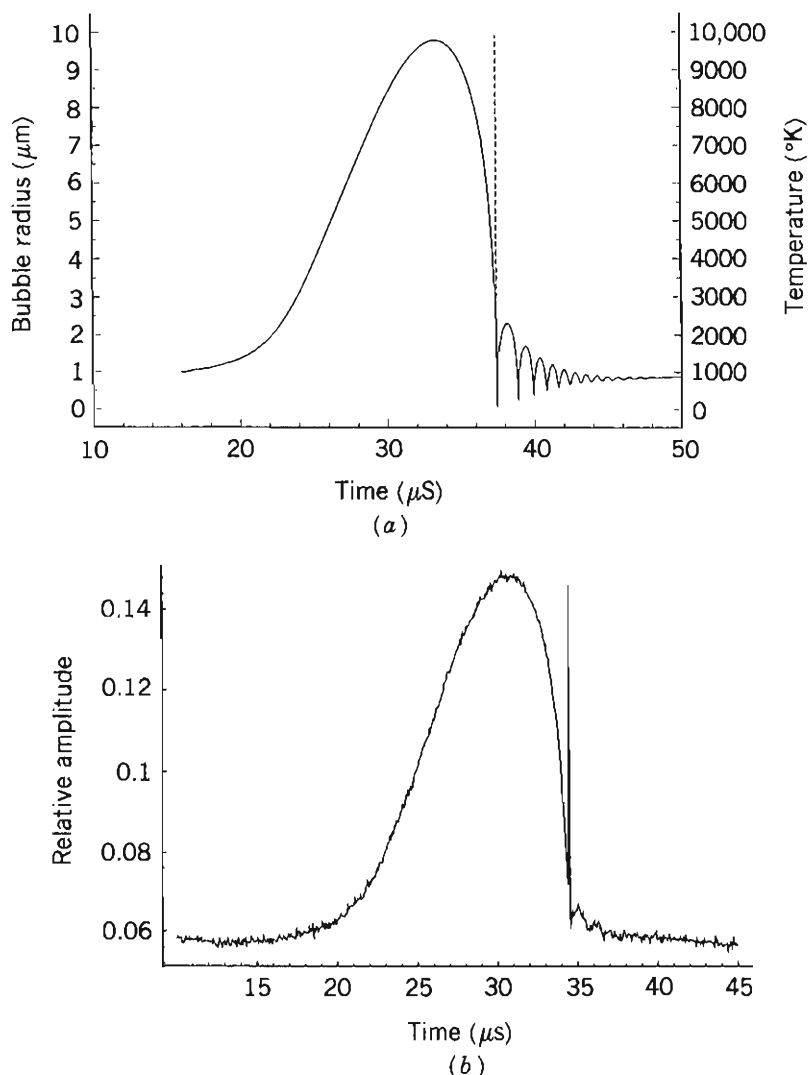


**Fig. 5** (a) Theoretical response of a single gas bubble when driven under conditions of SBSL (solid line). Pressure amplitude 0.136 MPa, equilibrium radius 4.5  $\mu\text{m}$ , and driving frequency 26.5 kHz. Bubble expands to several times its initial radius and then implodes. Broken line: calculation of the interior bubble temperature assuming an adiabatic collapse of the cavity contents. (Courtesy of John Allen.) (b) Measured response of a gas bubble to conditions similar to those shown. Experimentally determined bubble radius reconstructed from the square root of the scattered laser light intensity. Intensity spike near bubble collapse is not due to the laser but results from the sonoluminescence emissions. With some minor adjustments, the theoretical and experimental curves for the bubble radius can be made to coincide. (Courtesy of Tom Matula.)



where the initial radius of the bubble at time zero is  $R_0$ . The ambient pressure of the liquid is  $P_0$ , the surface tension  $\sigma$ , the shear viscosity  $\mu$ , and the polytropic exponent  $\gamma$ . The latter is set to 1.4 assuming the bubble behaves as an adiabatic system.

We can use the Gilmore equation to compute the behavior of a bubble undergoing SBSL for conditions similar to those in which this phenomenon is observed experimentally. Figure 5a shows an example of these computations. The solid line is the radius–time curve; the dashed line is the computed temperature in the interior of the bubble based upon the assumptions of this model.

It is possible to test experimentally certain aspects of these models. For example, using a light-scattering technique, various researchers have obtained measurements of the radius–time curve, simultaneous with the optical emissions,<sup>41,57</sup> as shown in Fig. 5b. Both the laser light scattered intensity and the SBSL can be acquired with a single photomultiplier tube. The SBSL emission is seen as the sharp spike in the figure, appearing at the final stages of bubble collapse. Note that these emissions occur at the point of minimum bubble size, as predicted by the hot-spot theory and that the general shape of the theoretical curve is reproduced. More quantitative assessment of these data has been made.<sup>57,58</sup>

The computations of single-bubble cavitation suggest

that the temperature of the gas within the bubble would remain at elevated temperatures for times on the order of tens of nanoseconds; however, there is strong evidence that the pulse duration of the SBSL flash is at least three orders of magnitude shorter than this value. The most plausible explanation for this short flash interval and some of the observed spectra (see below) is that an imploding shock wave is created within the gas bubble during the final stages of collapse. If this shock wave does indeed exist, exciting possibilities can be inferred about the temperatures that could be attained within the bubble and the physics that might result. Indeed, speculations on the possibilities of inertial confinement fusion have been made.<sup>59–61</sup>

#### 4.5 Spectroscopic Probes of Cavitation Conditions

Determination of the temperatures reached in a cavitating bubble has remained a difficult experimental problem. As a spectroscopic probe of the cavitation event, MBSL provides a solution. High-resolution MBSL spectra from silicone oil have been reported and analyzed.<sup>8</sup> The observed emission comes from excited state  $C_2$  and has been modeled with synthetic spectra as a function of rotational and vibrational temperatures, as shown in

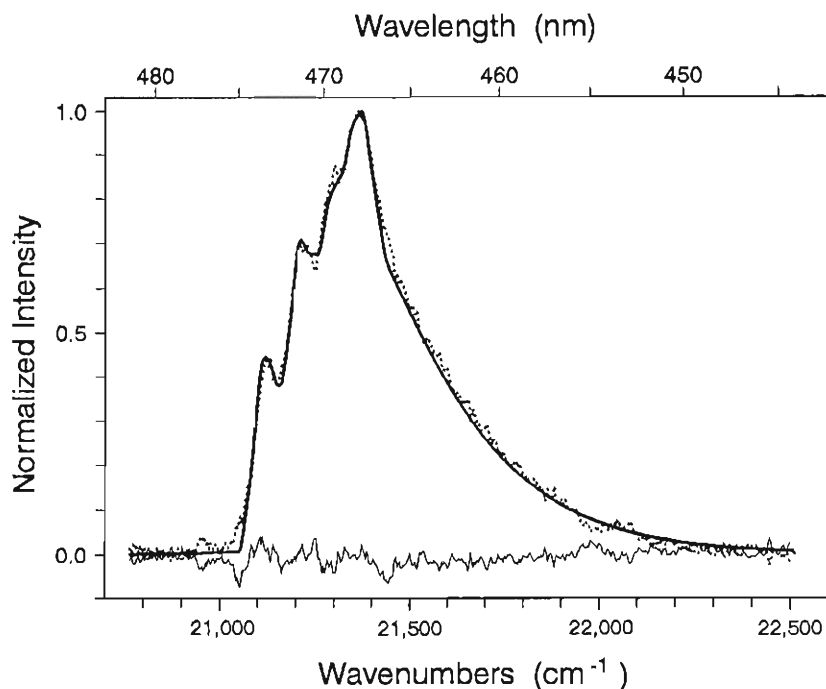


**Fig. 6** Sonoluminescence of excited state  $C_2$ . Emission from the  $\Delta v = +1$  manifold of the  $d^3\Pi_g - a^3\Pi_u$  transition (Swan band) of  $C_2$ . (·····) Observed sonoluminescence from silicone oil (polydimethylsiloxane, Dow 200 series, 50 cSt viscosity) under a continuous Ar sparge at 0°C. (—) Best fit synthetic spectrum, with  $T_v = T_r = 4900$  K. (---) Difference spectrum.

Fig. 6. From comparison of synthetic to observed spectra, the effective cavitation temperature is  $5050 \pm 150$  K. The excellence of the match between the observed MBSL and the synthetic spectra provides definitive proof that the sonoluminescence event is a thermal, chemiluminescence process. The agreement between this spectroscopic determination of the cavitation temperature and that made by comparative-rate thermometry of sonochemical reactions<sup>7</sup> is surprisingly close.

The interpretation of the spectroscopy of SBSL is much more unclear. Some very interesting effects are observed when the gas contents of the bubble are changed.<sup>55</sup> These results are shown in Fig. 7. Note that doping a nitrogen bubble with small quantities of noble gases drastically affects the emission intensity. Further-

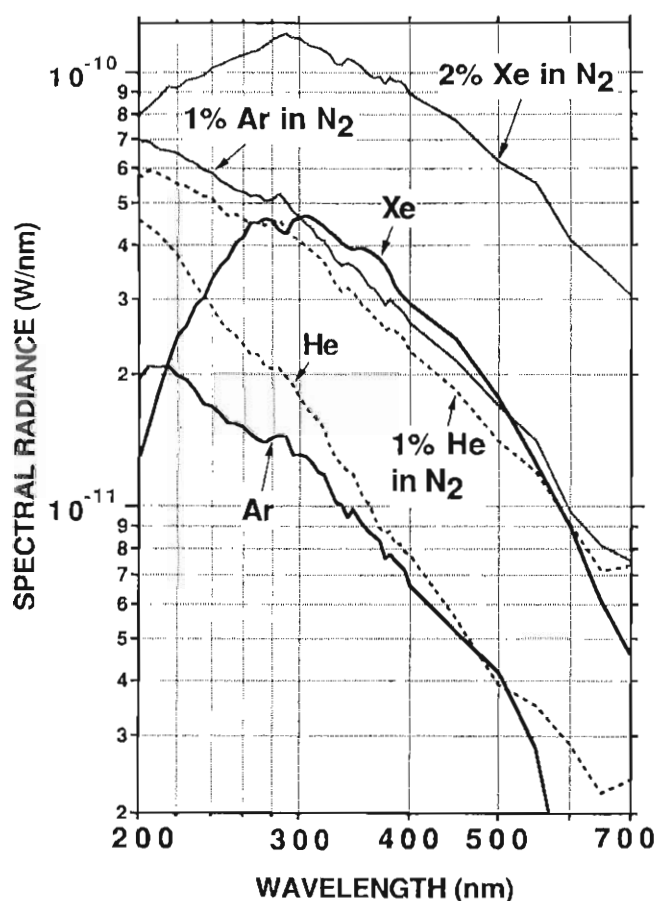


Fig. 7 Spectrum of SBSL for a variety of different gas mixtures in water. Pressure head 150 Torr. In contrast to spectra for MBSL, curves are relatively smooth and in some cases show a steady increase in intensity as one progresses to smaller wavelengths. Data have been corrected for the adsorption of water and quartz and for the quantum efficiency of the photodetector. (Reprinted with permission from Ref. 54. Copyright 1994 American Association for the Advancement of Science. Courtesy of Bob Hillier.)

more, the spectra show practically no evidence of OH emissions and, when He and Ar bubbles are considered, continue to increase in intensity for smaller and smaller wavelengths. These spectra suggest that temperatures considerably in excess of 5000 K may exist within the bubble and lend some support to the concept of an imploding shock wave. Several other alternative explanations for SBSL have been presented, and there exists considerable theoretical activity in this particular aspect of SBSL.<sup>62-66</sup>

### Acknowledgments

We acknowledge the support of the Office of Naval Research (L. A. C.), the National Institutes of Health through grant numbers DK43881 (L. A. C.) and HL25934 (K. S. S.), and the National Science Foundation through grant numbers CHE-9420758 and DMR-89-20538 (K. S. S.) and PHY-9311108 (L. A. C.).

### REFERENCES

1. K. S. Suslick (Ed.), *Ultrasound: Its Chemical, Physical, and Biological Effects*, VCH Publishers, New York, 1988.
2. K. S. Suslick, *Science*, Vol. 247, 1990, p. 1439.
3. T. J. Mason (Ed.), *Advances in Sonochemistry*, Vols. 1-3, JAI Press, New York, 1990, 1991, 1993.
4. T. J. Mason and J. P. Lorimer, *Sonochemistry: Theory, Applications and Uses of Ultrasound in Chemistry*, Ellis Horwood, Chichester, United Kingdom, 1988.
5. G. J. Price (Ed.), *Current Trends in Sonochemistry*, Royal Society of Chemistry, Cambridge, 1992.
6. O. V. Abramov, *Ultrasound in Liquid and Solid Metals*, CRC Press, Boca Raton, FL, 1994.
7. K. S. Suslick, D. A. Hammerton, and R. E. Cline, Jr., *J. Am. Chem. Soc.*, Vol. 108, 1986, p. 5641.
8. E. B. Flint and K. S. Suslick, *Science*, Vol. 253, 1991, p. 1397.
9. T. G. Leighton, *The Acoustic Bubble*, Academic, London, 1994, pp. 531-551.
10. S. J. Doktycz and K. S. Suslick, *Science*, Vol. 247, 1990, pp. 1067.
11. K. S. Suslick and S. J. Doktycz, *Adv. Sonochem.*, Vol. 1, 1990, pp. 197-230.
12. C. Einhorn, J. Einhorn, and J.-L. Luche, *Synthesis*, Vol. 1989, 1989, p. 787.
13. P. Boudjouk, *Comments Inorg. Chem.*, Vol. 9, 1990, p. 123.
14. J. M. Pestman, J. B. F. N. Engberts, and F. de Jong, *Recl. Trav. Chim. Pays-Bas*, Vol. 113, 1994, p. 533.
15. K. S. Suslick, "Sonochemistry of Transition Metal Compounds," in R. B. King (Ed.), *Encyclopedia of Inorganic Chemistry*, Vol. 7, 1996, Wiley, New York, pp. 3890-3905.

16. K. S. Suslick and D. J. Casadonte, *J. Am. Chem. Soc.*, Vol. 109, 1987, p. 3459.
17. L. A. Crum, *Physics Today*, Vol. 47, 1994, p. 22.
18. S. J. Putterman, *Sci. Am.*, February 1995, p. 46.
19. Lord Rayleigh, *Philos. Mag.*, Vol. 34, 1917, p. 94.
20. W. T. Richards and A. L. Loomis, *J. Am. Chem. Soc.*, Vol. 49, 1927, p. 3086.
21. M. A. Margulis, *Ultrasonics*, Vol. 30, 1992, p. 152.
22. T. Lepoint and F. Mullie, *Ultrasonics Sonochem.*, Vol. 1, 1994, p. S13.
23. A. Henglein, *Ultrasonics*, Vol. 25, 1985, p. 6.
24. A. Henglein, *Adv. Sonochem.*, Vol. 3, 1993, p. 17.
25. C. M. Preece and I. L. Hansson, *Adv. Mech. Phys. Surf.*, Vol. 1, 1981, p. 199.
26. W. Lauterborn and A. Vogel, *Ann. Rev. Fluid Mech.*, Vol. 16, 1984, p. 223.
27. J. R. Blake and D. C. Gibson, *Ann. Rev. Fluid Mech.*, Vol. 19, 1987, p. 99.
28. P. Riesz, *Adv. Sonochem.*, Vol. 2, 1991, p. 23.
29. M. A. Margulis and N. A. Maximenko, *Adv. Sonochem.*, Vol. 2, 1991, p. 253.
30. K. S. Suslick, J. W. Gawienowski, P. F. Schubert, and H. H. Wang, *J. Phys. Chem.*, Vol. 87, 1983, p. 2299.
31. K. S. Suslick, J. W. Goodale, H. H. Wang, and P. F. Schubert, *J. Am. Chem. Soc.*, Vol. 105, 1983, p. 5781.
32. K. S. Suslick, *MRS Bulletin*, Vol. 20, 1995, pp. 29–34.
33. K. S. Suslick, S. B. Choe, A. A. Cichowlas, and M. W. Grinstaff, *Nature*, Vol. 353, 1991, p. 414.
34. K. S. Suslick and M. W. Grinstaff, *J. Am. Chem. Soc.*, Vol. 112, 1990, p. 7807.
35. T. Ando and T. Kimura, *Adv. Sonochem.*, Vol. 2, 1991, p. 211.
36. J.-L. Luche *Ultrasonics Sonochem.*, Vol. 1, 1994, p. S111.
37. K. Chatakondou, M. L. H. Green, M. E. Thompson, and K. S. Suslick, *J. Chem. Soc. Chem. Commun.*, 1987, p. 900.
38. A. N. Mal'tsev, *Zh. Fiz. Khim.*, Vol. 50, 1976, p. 1641.
39. B. H. Han and P. Boudjouk, *Organometallics*, Vol. 2, 1983, p. 769.
40. H. Frenzel and H. Schultes, *Z. Phys. Chem.*, Vol. 27b, 1934, p. 421.
41. L. A. Crum, *J. Acoust. Soc. Am.*, Vol. 95, 1994, p. 559.
42. D. F. Gaitan and L. A. Crum, in M. Hamilton and D. T. Blackstock (Eds.), *Frontiers of Nonlinear Acoustics*, 12th ISNA, Elsevier Applied Science, New York, 1990, pp. 459–463.
43. D. F. Gaitan, L. A. Crum, R. A. Roy, and C. C. Church, *J. Acoust. Soc. Am.*, Vol. 91, 1992, p. 3166.
44. B. P. Barber and S. J. Putterman, *Nature*, Vol. 352, 1991, p. 318.
45. L. A. Crum and R. A. Roy, *Science*, Vol. 266, 1994, p. 233.
46. H. G. Flynn, "Physics of Acoustic Cavitation in Liquids," in W. P. Mason (Ed.), *Physical Acoustics*, Vol. IB, Academic, New York, 1964, p. 157.
47. L. A. Crum and J. B. Fowlkes, *Nature*, Vol. 319, 1986, p. 52.
48. L. A. Crum and D. F. Gaitan, *Proc. Int. Soc. Opt. Eng.*, Vol. 1161, 1989, p. 125.
49. L. A. Crum, R. A. Roy, M. A. Dinno, C. C. Church, R. E. Apfel, C. K. Holland, and S. I. Madanshetty, *J. Acoust. Soc. Am.*, Vol. 91, 1992, p. 1113.
50. R. E. Verrall and C. Sehgal, in K. S. Suslick (Ed.) *Ultrasound: Its Chemical, Physical, and Biological Effects*, VCH Publishers, New York, 1988, pp. 227–287.
51. E. B. Flint and K. S. Suslick, *J. Phys. Chem.*, Vol. 95, 1991, p. 1484.
52. E. B. Flint and K. S. Suslick, *J. Am. Chem. Soc.*, Vol. 111, 1989, p. 6987.
53. T. J. Matula, R. A. Roy, P. D. Mourad, W. B. McNamara III, and K. S. Suslick, submitted.
54. R. Hiller, K. Weninger, S. J. Putterman, and B. P. Barber, *Science*, Vol. 266, 1994, p. 248.
55. B. P. Barber, R. Hiller, K. Arisaka, H. Fetterman, and S. J. Putterman, *J. Acoust. Soc. Am.*, Vol. 91, 1992, p. 3061.
56. M. J. Moran et al., "Direct Observations of Single Sonoluminescence Pulses," *UCRL-JC-118486* (Preprint), Lawrence Livermore National Lab, October 1994.
57. B. P. Barber and S. J. Putterman, *Phys. Rev. Lett.*, Vol. 69, 1992, p. 3839.
58. R. Lofstedt, B. P. Barber, and S. J. Putterman, *Phys. Fluids*, Vol. A5, 1993, p. 2911.
59. B. P. Barber, C. C. Wu, R. Lofstedt, P. H. Roberts, and S. J. Putterman, *Phys. Rev. Lett.*, Vol. 72, 1994, p. 1380.
60. C. C. Wu and P. H. Roberts, *Phys. Rev. Lett.*, Vol. 70, 1993, p. 3424.
61. W. C. Moss, D. B. Clarke, J. W. White, and D. A. Young, *Phys. Fluids*, Vol. 6, 1994, p. 2979.
62. L. Frommhold and A. A. Atchley, *Phys. Rev. Lett.*, Vol. 73, 1994, p. 2883.
63. R. G. Holt, D. F. Gaitan, A. A. Atchley, and J. Holzfluss, *Phys. Rev. Lett.*, Vol. 72, 1994, p. 1376.
64. C. C. Wu and P. H. Roberts, *Proc. R. Soc. Lond. A*, Vol. 445, 1994, p. 323.
65. J. Schwinger, *Proc. Natl. Acad. Sci.*, Vol. 89, 1992, p. 4091.
66. V. Kamath, A. Prosperetti, and F. N. Egolfopoulos, *J. Acoust. Soc. Am.*, Vol. 94, 1993, p. 248.